

Rayleigh scattering, long-time tails, and the harmonic spectrum of topologically disordered systems

Carl Ganter

Institut für Radiologie, Technische Universität München, Ismaninger Str. 22, D-81675 München, Germany

Walter Schirmacher

Institut für Physik, Universität Mainz, D-55099 Mainz, Germany and Physik-Department E13,

Technische Universität München, D-85747 Garching, Germany

(Received 29 July 2010; revised manuscript received 25 August 2010; published 30 September 2010)

We show rigorously that a topologically disordered system interacting harmonically via force constants, which have a sufficiently short-ranged site-distance dependence, exhibits Rayleigh scattering in the low-frequency limit, i.e., a sound attenuation constant, which is proportional to ω^{d+1} , where ω is the frequency and d the dimensionality. This had been questioned in the literature. The corresponding nonanalyticity in the spectrum is related to a long-time tail in the velocity autocorrelation function of the analogous diffusion problem, which varies with time t as $t^{-(d+2)/2}$. A self-consistent theory for the spectrum is formulated, which has the correct analytical properties.

DOI: [10.1103/PhysRevB.82.094205](https://doi.org/10.1103/PhysRevB.82.094205)

PACS number(s): 05.40.-a, 63.50.-x

I. INTRODUCTION

Rayleigh scattering,¹ i.e., the fact that the elastic mean-free path of weakly scattered waves varies as $\omega^{-(d+1)}$ in a d -dimensional disordered medium as $\omega \rightarrow 0$, had been widely believed²⁻⁴ to be a general property of quenched disordered matter. This is so because elastic scattering of acoustic waves from frozen inhomogeneities in a disordered solid is analogous to the scattering of electromagnetic waves from inhomogeneities in the air. So the mathematics leading to the Rayleigh law was taken over.

However, recently it has been claimed⁵⁻⁸ that a harmonic system with “scalar displacements”⁹ $u_i(t)$ obeying

$$\frac{d^2}{dt^2}u_i(t) = - \sum_j t_{ij}[u_i(t) - u_j(t)], \quad (1)$$

where i and j denote random sites (positions) $\mathbf{r}_{i,j}$ in d -dimensional space, would have wavelike excitations, which have a linewidth Γ (proportional to the inverse mean-free path ℓ^{-1}), varying with ω^2 instead of ω^4 in $d=3$. t_{ij} are force constants, divided by the mass at the node i , which are assumed to depend on the distance, i.e., $t_{ij}=t(r_{ij})$. The authors make a distinction between systems which can be divided into a reference and perturbing part—such as a crystalline solid with defects—and those, in which such a distinction cannot be made—such as a glass or amorphous solid. They argue that the absence of such a distinction is the reason for the existence of a $\Gamma \propto \omega^2$ law instead of Rayleigh’s $\Gamma \propto \omega^4$ asymptotics, which they suppose to hold if a reference/defect separation can be made. The authors of Refs. 5–8 corroborate their claim of absence of Rayleigh scattering in a topologically disordered system by a theoretical analysis of the problem in Eq. (1), in which a high-density expansion and a diagrammatical analysis is performed.

Their claim is not only astonishing with respect to the mentioned general view on waves in disordered solids, but it is also in contradiction with the known analytic properties of

the analogous diffusion system. If one replaces the double time derivative in Eq. (1) by a single one, one obtains the equation of a random walk among the sites i, j

$$\frac{d}{dt}n_i(t) = - \sum_j t_{ij}[n_i(t) - n_j(t)], \quad (2)$$

where $n_i(t)$ gives the odds for the walker to be at i at time t and $t_{ij}=t(r_{ij})$ is the hopping probability per unit time. Equation (2) describes, e.g., the motion of electrons hopping among shallow impurities in a semiconductor.¹⁰⁻¹³ Such a random walk is known to exhibit a long-time tail of the velocity-autocorrelation function (VAF) varying as¹⁴⁻¹⁷

$$Z(t) \equiv \langle v_\alpha(t+t_0)v_\alpha(t_0) \rangle \propto t^{-(d+2)/2} \quad \text{for } t \rightarrow \infty, \quad (3)$$

a feature shared with Lorentz models.¹⁶⁻¹⁹ Here v_α is any Cartesian component of the random walker’s velocity. The Laplace transform of the VAF

$$D(s) = \int_0^\infty dt e^{-st} Z(t) \quad (4)$$

with $s=i\omega+\epsilon$ can be interpreted as a frequency-dependent diffusivity²⁰ because $D(s=0) \equiv D_0$ is the ordinary diffusion coefficient. As a consequence of the long-time tail the frequency-dependent part of $\Delta D(s) = D(s) - D_0$ has, according to the Tauberian theorems²¹ a low-frequency singularity $\Delta D(s) \rightarrow s^{d/2}, |s| \rightarrow 0$. Now, in the analogous vibrational problem, $D(s)$ corresponds to the square of a frequency-dependent sound velocity $v^2(s) \equiv D(s = -\omega^2 + i\epsilon)$. The imaginary part $v''(\omega)$ of $v(s)$ is related to the mean-free path $\ell(\omega)$ and the sound attenuation coefficient (Brillouin linewidth) $\Gamma(\omega)$ via

$$\frac{1}{\ell(\omega)} = \frac{2\omega v''(\omega)}{|v(s)|^2} = \frac{1}{2|v(s)|} \Gamma(\omega). \quad (5)$$

This gives $\Gamma(\omega) \propto \omega^{d+1}$, i.e., Rayleigh scattering. We conclude that the long-time tail of the VAF in the diffusion prob-

lem is mathematically equivalent to the Rayleigh-scattering property.²²

There exists a further mathematical analogy. Via the Einstein-Nernst relation the frequency-dependent diffusivity $D(s=i\omega+\epsilon)$ is proportional to the dynamic conductivity $\sigma(\omega)$. Therefore, the low-frequency nonanalyticity of $D(s)$ leads to a low-frequency behavior of the ac conductivity $\Delta\sigma(\omega)=\text{Re}\{\sigma(\omega)-\sigma(0)\}\propto\omega^{d/2}$. So, if the authors of Refs. 5–8 would be right, $\Delta\sigma(\omega)$ should vary as $\Delta\sigma(\omega)\propto\omega^{(d-2)/2}$ instead. Both in measured²³ ($d=3$) and simulated²⁴ ($d=2$) ac hopping conductivity data the $\Delta\sigma(\omega)\propto\omega^{d/2}$ behavior can be unambiguously identified.

In the following we apply the methods of Ernst *et al.*¹⁶ and Machta *et al.*¹⁷ in order to show rigorously that a system governed by Eq. (2) with sufficiently fast decaying quantities $t(r)$ behaves as $D(s)\propto s^{d/2}$ for $s\rightarrow 0$ and *not* $D(s)\propto s^{(d-2)/2}$ as claimed by the quoted authors. In the second part of the present contribution we formulate a self-consistent theory for the spectral properties of a topologically disordered system governed by Eq. (1) and (2), which has the correct analytical properties.

II. NONANALYTIC SELF-ENERGY AND LONG-TIME TAIL

We start by studying the random walk in Eq. (2). It has been shown^{10,11} that this problem can be mapped onto a *random-resistor network* problem, in which the sites i are connected with conductances $g_{ij}\propto t_{ij}$. For a given box with volume V_c the conductance of the network inside the box and hence the conductivity and diffusivity can be calculated.^{12,13,25} We call this diffusivity $D_{V_c}(\mathbf{r})$, where \mathbf{r} is the vector pointing to the center of the box. For $V_c\rightarrow\infty$ we have $D_{V_c\rightarrow\infty}=D_0$, which is the macroscopic diffusivity. Tiling the total volume V into smaller boxes of volume V_c we arrive at a coarse-grained system with a *spatially fluctuating diffusivity* obeying the following equation of motion for the continuous density $n(\mathbf{r}, t)$:

$$\frac{\partial}{\partial t}n(\mathbf{r}, t) = \nabla D_{V_c}(\mathbf{r}) \nabla n(\mathbf{r}, t). \quad (6)$$

The fluctuations of D_{V_c} arise because of the different arrangements of sites inside of the coarse-graining boxes. For large volumes V_c the point statistics enters the diffusivity only via the density [see Refs. 12, 13, and 25, and the second part of this article]. This means that the variance of D_{V_c} can be written

$$\langle(\Delta D_{V_c})^2\rangle = \left[\frac{\partial D_{V_c}}{\partial \rho_c}\right]^2 \langle(\Delta \rho_c)^2\rangle, \quad (7)$$

where $\rho_c=N_c/V_c$ and N_c is the actual number of particles inside a coarse-graining volume. The statistics of N_c is for large N_c Poissonian,²¹ i.e., the variance of N_c is equal to its mean ρV_c . From this it follows that the variance of ρ_c and hence that of D_{V_c} is inversely proportional to V_c , and we can write $\langle(\Delta D_{V_c})^2\rangle=\sigma'/V_c$, where σ' is the fluctuation density. In the long-wavelength limit we may increase the size of V_c

proportional to the wavelength. We are then allowed to use the variance $\langle\Delta D_{V_c}^2\rangle$ as small parameter.²⁶

In the Laplace-transformed domain the Green's function corresponding to Eq. (6) obeys the equation of motion

$$\{s - \nabla[D_0 + \Delta D_{V_c}(\mathbf{r})]\nabla\}G(\mathbf{r}, \mathbf{r}', s) = \delta(\mathbf{r} - \mathbf{r}') \quad (8)$$

from which the following recursion formula^{16,27} for

$$G(\mathbf{k}, \mathbf{k}', s) = \frac{1}{V} \int d\mathbf{r} \int d\mathbf{r}' e^{-i\mathbf{k}\mathbf{r}} e^{i\mathbf{k}'\mathbf{r}'} G(\mathbf{r}, \mathbf{r}', s) \quad (9)$$

can be derived

$$G(\mathbf{k}, \mathbf{k}', s) = G_0(k, s) \delta_{\mathbf{k}, \mathbf{k}'} - \int \left(\frac{d\mathbf{q}}{2\pi}\right)^d \mathbf{k} \cdot \mathbf{q} \Delta D_{V_c}(\mathbf{k} - \mathbf{q}) G(\mathbf{q}, \mathbf{k}', s) \quad (10)$$

with

$$\Delta D_{V_c}(\mathbf{k}) = \int d\mathbf{r} e^{-i\mathbf{k}\mathbf{r}} \Delta D_{V_c}(\mathbf{r}). \quad (11)$$

Here

$$G_0(k, s) = [s + D_0 k^2] \quad (12)$$

is the ‘‘unperturbed’’ Green's function. We represent now the averaged Green's function in terms of a self-energy function $\Sigma(\mathbf{k}, s)$ as

$$\begin{aligned} \langle G(\mathbf{k}, \mathbf{k}', s) \rangle &= \delta_{\mathbf{k}, \mathbf{k}'} \frac{1}{G_0^{-1}(k, s) - \Sigma(\mathbf{k}, s)} \Leftrightarrow \Sigma(\mathbf{k}, s) \\ &= \frac{1}{G_0(k, s)} - \frac{1}{\langle G(\mathbf{k}, \mathbf{k}', s) \rangle_{\mathbf{k}=\mathbf{k}'}}. \end{aligned} \quad (13)$$

Iterating Eq. (10) twice and expanding the fraction in Eq. (13) to second order in the fluctuations we obtain (using $\langle\Delta D_{V_c}\rangle=0$)

$$\Sigma(\mathbf{k}, s) = \frac{1}{(2\pi)^d} \int d^d\mathbf{p} K_{V_c}(\mathbf{k} - \mathbf{p}) (\mathbf{k} \cdot \mathbf{p})^2 G_0(\mathbf{p}, s), \quad (14)$$

where

$$K_{V_c}(\mathbf{k}) = \int d^d\mathbf{r} e^{i\mathbf{k}\mathbf{r}} \langle \delta D_{V_c}(\mathbf{r}_0 + \mathbf{r}) \delta D_{V_c}(\mathbf{r}_0) \rangle \quad (15)$$

is the Fourier-transformed correlation function of the diffusivity fluctuations. For $t(r)$ falling off rapidly enough with distance r $K_{V_c}(0)$ is finite²⁸ and we can write

$$K_{V_c}(\mathbf{k}) = \sigma' f_{V_c}(k) \quad (16)$$

with $f_{V_c}(k)=1$ for $k < k_c=2\pi/V_c^{1/d}$ and 0 elsewhere. Equation (14) is the *Born approximation* for the coarse-grained hopping problem.

In the long-wavelength limit $k\rightarrow 0$ we obtain

$$\Sigma(\mathbf{k}, s) \propto k^2 \sigma' \int_0^{k_c} dp \frac{p^{d+1}}{s + Dp^2}. \quad (17)$$

If we define

$$D(s) = v^2(s) = D_0 - \lim_{k \rightarrow 0} \frac{1}{k^2} \Sigma(k, s) \quad (18)$$

we obtain for $|s| \rightarrow 0$ from Eq. (17) a contribution to $D(s)$, which is nonanalytic in the complex variable s , namely,

$$\Delta D(s) \propto s^{d/2}, \quad (19)$$

which implies

$$\Gamma(\omega) \propto \ell^{-1}(\omega) \propto \omega^{d+1} \quad \text{for } \omega \rightarrow 0 \quad (20)$$

and

$$Z(t) \propto t^{-(d+2)/2} \quad \text{for } t \rightarrow \infty. \quad (21)$$

This completes our proof. Of course this proof holds also for any other inhomogeneous system (due to quenched disorder) allowing for a nonvanishing diffusivity in the limit $V_c \rightarrow \infty$.^{16,17} It is interesting to note that the nonanalyticity is a case of *generic scale invariance*, which appears frequently in many-body systems, especially near phase transitions.²⁹ In the present case this phenomenon is due to the particle conservation in the diffusion problem and momentum conservation in the phonon problem.

III. EUCLIDEAN RANDOM-MATRIX APPROACH

We now turn to an approximate solution of the problem posed in Eq. (1), or, equivalently in Eq. (2). Approximate theories for solving problems of the type of Eq. (2) have a long history.^{12,13} However, they all suffer from the absence of the correct nonanalyticity. We show in the following, how a self-consistent theory with the correct analytic properties is derived.

A. High-density diagrammatic expansion of the self-energy

As in Refs. 5 and 6 we start from a high-frequency (s) and high-density ($\rho = N/V$) expansion of the averaged propagator

$$\begin{aligned} G(\mathbf{k}, s) &= \frac{1}{N} \sum_{mn} \langle e^{i\mathbf{k}\mathbf{r}_{mn}} [s\mathbf{1} - \mathbf{M}]_{mn}^{-1} \rangle \\ &= \frac{1}{s} + \sum_{p=1}^{\infty} \frac{1}{s^{p+1}} \frac{1}{N} \sum_{i_0 \dots i_p} \langle e^{i\mathbf{k}\mathbf{r}_{i_0 i_1}} M_{i_0 i_1}, \dots, e^{i\mathbf{k}\mathbf{r}_{i_{p-1} i_p}} M_{i_{p-1} i_p} \rangle \\ &= \frac{1}{s - \rho[t(k) - t(0)] - \Sigma(\mathbf{k}, s)}. \end{aligned} \quad (22)$$

Here \mathbf{M} is a matrix with off-diagonal elements $M_{ij} = t_{ij}$ and diagonal elements $M_{ii} = -\sum_{\ell \neq i} t_{i\ell}$. In the case of a random site distribution (which we assume) $t(k) = t(\mathbf{k})$ is the d -dimensional Fourier transform of $t(r)$. The self-energy $\Sigma(\mathbf{k}, s)$ is the sum of all irreducible diagrams with respect to $e^{i\mathbf{k}\mathbf{r}_{mn}} M_{mn}$ and $G_0(\mathbf{k}, s) = [s - \rho[t(k) - t(0)]]^{-1}$. They are grouped with respect to increasing order in ρ^{-1} , i.e.,

$$\Sigma(\mathbf{k}, s) = \sum_{\nu=1}^{\infty} \Sigma_{\nu} \rho^{-\nu}. \quad (23)$$

The frequency-dependent diffusivity is given by

$$D(s) = -\frac{1}{2} \frac{\partial^2}{\partial k^2} [t(k) + \Sigma(k, s)]_{k \rightarrow 0}. \quad (24)$$

The first-order self energy is identical to that given in Refs. 5 and 6, namely,

$$\Sigma_1(\mathbf{k}, s) = \rho \int \left(\frac{d\mathbf{p}}{2\pi} \right)^d [t(\mathbf{k} - \mathbf{p}) - t(\mathbf{p})]^2 G_0(p, s). \quad (25)$$

This gives, in accord with^{5,6} $\Sigma_1''(\mathbf{k}, s) \propto k^2 s^{3/2}$.

In order to reveal the analytic properties of the second-order self-energy it is important to observe the order of repeated site indices appearing in the summation of terms (diagrams) in Eq. (22). The arrangement of the repeated indices determines the topological structure of the diagrams. As shown in Refs. 6 and 30 there are three main topologically different sets of diagrams: (a) diagrams with a twofold repetition of indices of the form (1-2-2-1), where “1” means the first index and “2” the second index. These diagrams have been called “cactus diagrams”⁶ because their iteration looks like a cactus. (b) Diagrams with a twofold repetition of indices of the form (1-2-1-2), called “crossed diagrams.” (c) Diagrams with a threefold repetition of indices (1-1-1).

A detailed analysis³⁰ shows that the “cactus” and “crossed” sets of diagrams can each be subdivided into two classes, namely, into eight diagrams in which the sequence of indices starts with a “direct” connection (i.e., by a factor t_{12} ,—notation: (12-2-1)—where, again 1 is the first and 2 is the second repeated index), and into 16 diagrams with an indirect connection—notation: (1*2-2-1). The (1-1-1) set comprises four diagrams and forms its own class. We define the five contributions to the second-order self-energy Σ_2 corresponding to the five classes as

$\Sigma_2^{(\alpha)} := (1*2-2-1):$	Sum of 16 diagrams
$\Sigma_2^{(\beta)} := (12-2-1):$	Sum of 8 diagrams
$\Sigma_2^{(\gamma)} := (1*2-1-2):$	Sum of 16 diagrams
$\Sigma_2^{(\delta)} := (12-1-2):$	Sum of 8 diagrams
$\Sigma_2^{(\epsilon)} := (1-1-1):$	Sum of 4 diagrams
Σ_2	Total Sum of 52 diagrams

It now turns out that the self-energies $\Sigma_2^{(\alpha)}, \dots, \Sigma_2^{(\epsilon)}$ separately obey the law

$$\lim_{k \rightarrow 0} [\Sigma_2^{(\mu)}]'' \propto k^2 s^{d/2} \quad \mu = \alpha, \dots, \epsilon \quad (26)$$

whereas each single diagram behaves as $k^2 s^{(d-2)/2}$ in the long-wavelength limit. The cancellation of the $k^2 s^{(d-2)/2}$ singularities can be traced to the column and row sum rule of the dynamical matrix

$$\sum_m M_{mn} = \sum_n M_{mn} = 0, \quad (27)$$

which in the diffusion problem arises from particle conservation, in the phonon problem from momentum conservation (or, equivalently, from global translational invariance). We conclude that to second order in ρ^{-1} the general Rayleigh-type singularity property required by Eqs. (17) and (19) is obeyed.

B. Self-consistent theory for the spectrum

We turn now to the formulation of a self-consistent approximation scheme, which amounts to a partial summation to all orders. In their approximation scheme Grigera *et al.* and Martín-Mayor *et al.*^{5,6} have replaced the zeroth-order propagator in Eq. (25) by the full propagator in Eq. (22), which constitutes a self-consistent set of equations. They claim to have summed all cactus-type diagrams. However, if one expands the self-energy given by this scheme to second order in the inverse density, one finds³⁰ that the 24 second-order diagrams are not identical to the 16+8 cactus diagrams $\Sigma_2^{(\alpha)} + \Sigma_2^{(\beta)}$, defined above. Instead, the summation comprises all diagrams in $\Sigma_2^{(\alpha)}$ but only an incomplete subset (four of eight) of diagrams from $\Sigma_2^{(\beta)}$ and $\Sigma_2^{(\delta)}$, respectively. Therefore, within this scheme the subtle cancellation leading to Eq. (26) does not take place and as a result an erroneous $\Sigma''(\mathbf{k}, s) \propto k^2 s^{(d-2)/2}$ behavior is obtained, which is an artifact of this self-consistent scheme.

In order to derive an analytically correct partial summation, based on cactus diagrams, several conditions have to be met: (a) to first order in ρ^{-1} the result should be the exact Σ_1 . (b) To second order in ρ^{-2} the self-energy should comprise a complete class of diagrams. (c) All higher orders $\propto \rho^{-n}$, with $n > 2$, must also yield a $s^{d/2}$ singularity.

As a solution to these demands, we propose the following self-consistent set of equations for calculating $\Sigma(\mathbf{k}, s)$:

$$\begin{aligned} \Sigma(\mathbf{k}, s) &= \int \left(\frac{d\mathbf{p}}{2\pi} \right)^d [t(\mathbf{k} - \mathbf{p}) - t(p)] g(p, s) \\ &\quad \times [\rho t(\mathbf{k} - \mathbf{p}) - \rho t(p) - \sigma(p, s) + \sigma(\infty, s)], \end{aligned} \quad (28a)$$

$$\begin{aligned} \sigma(\mathbf{k}, s) &= \rho \int \left(\frac{d\mathbf{p}}{2\pi} \right)^d [t(\mathbf{k} - \mathbf{p}) - t(p)] \\ &\quad \times [t(\mathbf{k} - \mathbf{p}) - t(k)] g(p, s), \end{aligned} \quad (28b)$$

$$g(k, s) = \frac{1}{s - \rho[t(k) - t(0)] - \sigma(k, s)}. \quad (28c)$$

The first two requirements can be verified easily by expanding $\Sigma(\mathbf{k}, s)$ up to ρ^{-2} : to lowest order in ρ^{-1} , Eq. (25) is obtained, and to second order the entire sums $\Sigma_2^{(\alpha)} + \Sigma_2^{(\beta)}$ are included, the other ones not. The validity of the third condition follows from a more subtle mechanism: it is important to note that the $s^{d/2}$ singularity of the exact self-energy $\Sigma(\mathbf{k}, s)$ is observed in the long-wavelength limit $k \rightarrow 0$ only,

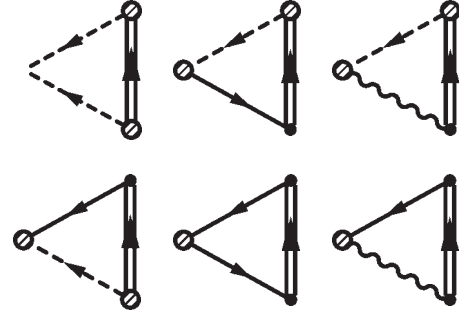


FIG. 1. Diagrammatic representation of $\Sigma(k, s)$ in the cactus-2 scheme. Solid and dashed lines represent t_{ij} factors, associated with off-diagonal and diagonal matrix elements of \mathbf{M} , respectively. The wiggled line stands for $\sigma(r_{ij}, s)$ and the double line for $g(r_{ij}, s)$. Open circles denote start and end points of the directed graph. The simpler cactus-1 scheme is obtained after omitting the two diagrams in the third column.

cf. Eqs. (17) and (19). For finite and nonzero values of k , $\Sigma''(\mathbf{k}, s)$ will, in general, show a $s^{(d-2)/2}$ singularity.³¹

This makes clear, why any self-consistent scheme, which contains an integral over a full propagator, as, e.g., done in Ref. 5 by inserting Eq. (17) into Eq. (25), is at least likely to spoil the $s^{d/2}$ law. While the diffusion pole produces a $s^{d/2}$, the remaining principle-value integral will—in general³²—contribute a $s^{(d-2)/2}$ term.

Therefore, the auxiliary propagator $g(k, s)$ instead of $G(k, s)$, enters the integrals in the scheme above. Unlike $\Sigma(k, s)$, the imaginary part of $\sigma(k, s)$ —and thus $g(k, s)$ —has a singularity $\propto s^{d/2}$ for all k .

It is straightforward to show that this in turn is a consequence of the slight structural difference between Eqs. (25) and (28b), namely, the replacement

$$[t(\mathbf{k} - \mathbf{p}) - t(p)]^2 \rightarrow [t(\mathbf{k} - \mathbf{p}) - t(p)][t(\mathbf{k} - \mathbf{p}) - t(k)]. \quad (29)$$

As stated above, this self-consistent scheme comprises the two cactus classes α and β to second order in ρ^{-1} , and we call it cactus-2. A simplified approximation, which only includes $\Sigma_2^{(\alpha)}$ to second order (called “cactus-1”) is obtained by dropping the σ terms in Eq. (28a).

Figures 1 and 2 give a diagrammatic interpretation of the cactus-1 and cactus-2 schemes. With respect to the latter,

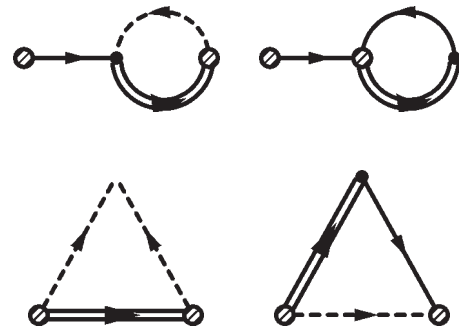


FIG. 2. Diagrammatic representation of $\sigma(k, s)$, i.e., the wiggled line in Fig. 1.

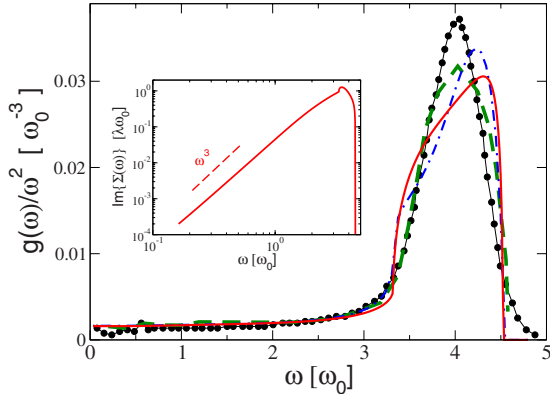


FIG. 3. (Color online) Reduced DOS $g(\omega)/\omega^2$ for $\rho=\lambda^{-3}$. Symbols: simulation (Ref. 5), green dashes: “old” cactus approximation (Ref. 5), blue dash dots: cactus-1 approximation, red full line: cactus-2 approximation. The frequency unit is $\omega_0=[\rho t_0]^{1/2}$. Insert: imaginary part of the self-energy $\Sigma(\omega)=\Sigma(k,\omega)/k^2|_{k\rightarrow 0}$, exhibiting the ω^3 law (calculated in cactus-1 approximation).

note that in the bracket in Eq. (28a), $\sigma(\infty,s)$ must be subtracted from $\sigma(p,s)$ to retain the irreducibility of the diagrams in the third column of Fig. 1.

Note that the $s^{(d-2)/2}$ singularities are balanced out in every column of Fig. 2 already. Therefore, cactus-1 and cactus-2 are not the only possible self-consistent sets of equations to yield a $s^{d/2}$ in all orders of the ρ^{-1} expansion.

As in Refs. 5–8 the density of states is given by

$$g(\omega) = \frac{2\omega}{\pi} \text{Im} \left\{ \lim_{k \rightarrow \infty} G(k,s) \right\}_{s=-\omega^2+i\epsilon}. \quad (30)$$

In Fig. 3 we have plotted the reduced three-dimensional density of states (DOS) $g(\omega)/\omega^2$ for Gaussian force constants $t(r)=t_0 e^{-r^2/2\lambda^2}$ for the density $\rho=\lambda^{-3}$ together with the numerical results presented in Ref. 5. While the overall agreement is not as good as for the cactus scheme of Ref. 5, we have obtained self-consistent equations which include the correct low-frequency nonanalyticity. To show this we have plotted in the inset of Fig. 3 double logarithmically the imaginary part of the self-energy, divided by k^2 , which is proportional to the imaginary part $v''(\omega)$ of the frequency-dependent sound velocity. The ω^3 behavior leads to the correct ω^4 law for the mean-free path and the sound attenuation coefficient. We observe that the Rayleigh regime with $\Sigma'' \propto \omega^3$ is ended by a steplike increase in ℓ^{-1} at a frequency quite below the upper band edge. In phenomenological models with spatially fluctuating elastic constants,^{33,34} such a feature indicates the crossover between wavelike and random-matrixlike excitations and has been identified as the reason for the frequently observed enhancement of the vibrational DOS over the Debye one (boson peak) (see the remarks in the conclusion).

All three cactus schemes exhibit for low-enough densities an instability. Such an instability usually occurs for force-constant distributions if one allows for negative values of t_{ij} [e.g., a Gaussian distribution $P(t_{ij})$].^{8,33,34} In the present case the force constants are positive definite and the instability is an artifact of the cactus approximation.

As stated in the beginning, at low density, i.e., in the strong-disorder limit, percolative aspects become important, which can be included by resummation techniques, which take repeated backward and forward hops into account.^{35,36} We shall show in a forthcoming paper that the instability disappears if the resummation is carried out.

IV. CONCLUSIONS

In conclusion we showed rigorously that a topologically disordered network consisting of harmonic springs and masses at the nodes exhibits Rayleigh scattering $\Gamma(\omega) \propto \omega^{d+1}$ if the distance dependence of the springs or their spatial correlations are short-ranged enough, i.e., the Fourier-transformed correlation function $K_V(k)$ is finite in the long-wavelength limit $k \rightarrow 0$. The Rayleigh-scattering property of the waves in a quenched-disordered environment is due to a nonanalyticity of the disorder-induced self-energy $\Sigma(k,s) \propto k^2 s^{s/2}$, which, in the mathematically equivalent diffusion problem gives rise to a long-time tail of the velocity autocorrelation function of the form $Z(t) \propto t^{-(d+2)/2}$. Our proof differs from that given in Refs. 16 and 17 by the coarse-graining procedure leading from Eqs. (1) and (2) to Eq. (6). Our procedure does not involve an average over the parameters t_{ij} but calculating the exact diffusivity within a coarse-graining volume.

In the second part of the present investigation we use the Euclidean random-matrix approach, which involves a high-frequency, high-density expansion of the resolvent of the problem in Eqs. (1) and (2). To second order in the inverse density we show that the self-energy exhibits the $\Sigma(k,s) \propto k^2 s^{s/2}$ singularity in contrast to the claims in Refs. 5–8. Furthermore we show that the self-consistent cactus approximation proposed by these authors does not obey the correct nonanalytical law because a subtle sum rule imposed by the column or row sum rule of the dynamical matrix was not taken care of. We proposed two self-consistent schemes, which have the correct analytic properties and which lead to reasonable agreement with a numerical evaluation of the spectrum.

Finally we would like to comment on the vibrational spectrum of a *real* topologically disordered solid. Such a spectrum differs qualitatively and quantitatively from that of the model discussed in the present paper. First of all, in a real solid the vibrational displacements are vector entities so that the generalization of Eq. (1) (Ref. 7) must be used. But, more important, the functional form of t_{ij} must be derived from a realistic interatomic pair potential and the statistics of the atomic sites must obey that dictated by this pair potential. A calculation using a suitable version of the coherent-potential approximation for glassy Lennard-Jones (LJ) Argon, in which the $t(r_{ij})$ and the pair distribution of the sites were compatible with the LJ potential, has been shown by the present authors to give results that agree with the corresponding molecular-dynamics results.³⁷ While such a theoretical approach for a system, in which the underlying potential is known, is very satisfactory, most glassy solids, which are investigated experimentally, cannot be modeled in terms of simple two-body potentials (see, however Ref. 38 and

references therein for the case of glassy SiO₂). For this general class of glassy solids it proved more reasonable not to take an equation of motion of type Eq. (1) as starting point, but, instead, a generalized-elasticity approach, in which the disorder enters via spatially fluctuating elastic constants [as in the schematic Eq. (6)]. A field-theoretically motivated mean-field theory (self-consistent Born approximation) applied to this model³⁴ showed that the frequently observed enhancement of the vibrational DOS over the Debye one (boson peak) marks the crossover between wavelike and random-matrixlike states, which occurs with increasing frequency. In the harmonic sound attenuation this crossover results in a change from a Rayleigh ω^4 law to a much weaker ω^s law with $s \approx 2$. This approach involves as input the statistics of the elastic constants, e.g., their variance and correlation length. Compared to the microscopical treatment this approach is much more modest, as it only qualitatively explains the salient features of the vibrational spectrum of disordered solids.

Another important remark concerns the role of anharmonic interactions. These interactions give rise to a temperature-dependent scattering rate^{39–41} low-frequency

$\Gamma_{\text{anh}} \propto T\omega^2$ so that it always dominates the low-frequency scattering at finite temperatures. However, there may exist a window in which the Rayleigh law can be observed. This window, unfortunately, lies in a frequency range (~ 100 GHz), which is not easily accessible by the existing light and x-ray scattering techniques. The existence of a Rayleigh regime in glassy SiO₂ has been recently a subject of intense investigations.^{42–44} At elevated temperatures the boson peak in this material shifts upwards in frequency due to a softening of elasticity.^{44,45} This moves the Rayleigh window into the frequency regime accessible by inelastic x-ray scattering so that there is now experimental evidence⁴⁴ for the observation of Rayleigh scattering in a topologically disordered material.

ACKNOWLEDGMENTS

We are grateful for helpful discussions with Kurt Binder, Thomas Franosch, Giancarlo Ruocco, Rolf Schilling, and Friederike Schmid. C.G. acknowledges gratefully hospitality in Mainz by Rolf Schilling.

-
- ¹J. W. Strutt (Lord Rayleigh), *Philos. Mag.* **41**, 247 (1871); **47**, 375 (1899); [reprint in Lord Rayleigh, *Scientific papers*, **1**, 87 (1899); **4**, 397 (1903)].
- ²P. G. Klemens, *Proc. R. Soc. London, Ser. A* **208**, 108 (1951).
- ³E. Akkermans and R. Maynard, *Phys. Rev. B* **32**, 7850 (1985).
- ⁴S. R. Elliott, *Europhys. Lett.* **19**, 201 (1992).
- ⁵T. S. Grigera, V. Martín-Mayor, G. Parisi, and P. Verrocchio, *Phys. Rev. Lett.* **87**, 085502 (2001).
- ⁶V. Martín-Mayor, M. Mézard, G. Parisi, and P. Verrocchio, *J. Chem. Phys.* **114**, 8068 (2001).
- ⁷S. Ciliberti, T. S. Grigera, V. Martín-Mayor, G. Parisi, and P. Verrocchio, *J. Chem. Phys.* **119**, 8577 (2003).
- ⁸T. S. Grigera, V. Martín-Mayor, G. Parisi, and P. Verrocchio, *J. Phys.: Condens. Matter* **14**, 2167 (2002); *Nature (London)* **422**, 289 (2003).
- ⁹The present argumentation also holds for more realistic models with vector displacements.
- ¹⁰A. Miller and E. Abrahams, *Phys. Rev.* **120**, 745 (1960).
- ¹¹V. Ambegaokar, B. I. Halperin, and J. S. Langer, *Phys. Rev. B* **4**, 2612 (1971).
- ¹²B. L. Shklovskii and A. L. Efros, *Electronic Properties of Doped Semiconductors* (Springer, Berlin, 1984).
- ¹³H. Böttger and V. V. Bryksin, *Hopping Conduction in Solids* (Akademie-Verlag, Berlin, 1985).
- ¹⁴J. Haus, K. W. Kehr, and K. Kitahara, *Z. Phys. B* **50**, 161 (1983).
- ¹⁵P. B. Visscher, *Phys. Rev. B* **29**, 5472 (1984).
- ¹⁶M. H. Ernst, J. Machta, J. R. Dorfman, and H. van Beijeren, *J. Stat. Phys.* **34**, 477 (1984).
- ¹⁷J. Machta, M. H. Ernst, H. van Beijeren, and J. R. Dorfman, *J. Stat. Phys.* **35**, 413 (1984).
- ¹⁸M. H. Ernst and A. Weyland, *Phys. Lett. A* **34**, 39 (1971).
- ¹⁹F. Höfling, T. Franosch, and E. Frey, *Phys. Rev. Lett.* **96**, 165901 (2006).
- ²⁰Note that the quantity $D(t)$ of Ref. 17 is defined by $D(t) = \int_0^t d\tau Z(\tau)$. The Laplace transform of this quantity is equal to $D(s)/s$, from which follows $D(t \rightarrow \infty) = D_0$.
- ²¹W. Feller, *An Introduction to Probability Theory and Its Applications* (Wiley, New York, 1950).
- ²²There exist further analogies, namely, to spin-wave scattering in disordered ferromagnets ($\ell \propto \omega^{-(d/2+1)}$) and antiferromagnets ($\ell \propto \omega^{-(d+1)}$), see Ref. 46.
- ²³A. R. Long, J. McMillan, N. Balkan, and S. Summerfield, *Philos. Mag.* **58**, 153 (1988).
- ²⁴W. F. Pasveer, P. A. Bobbert, and M. A. J. Michels, *Phys. Rev. B* **74**, 165209 (2006).
- ²⁵J. A. McInnes, P. N. Butcher, and J. D. Clark, *Philos. Mag. B* **41**, 1 (1980).
- ²⁶This argumentation, of course, holds only for independent fluctuations ΔD_{V_c} . This excludes the vicinity of a phase transition or a percolation transition. In such a case the correlation length must be at least smaller than the wavelength (in the sound case) for a given frequency or the mean-square displacement (in the diffusion case) for a given time. In the case of a Lorentz model, which exhibits a percolation transition, a crossover from the Rayleigh-type long-time tail to a critical tail has been observed (Ref. 19).
- ²⁷We use periodic boundary conditions for the plane waves normalized in the total volume V .
- ²⁸This includes force constants derived from Lennard-Jones-type potentials. $\Sigma \propto k^2 s^{d/2}$ breaks down for cases in which $K(k)$ becomes critical for $k \rightarrow 0$, i.e., near phase transitions or for long-range interactions $t(r)$.
- ²⁹D. Belitz, T. Kirkpatrick, and T. Vojta, *Rev. Mod. Phys.* **77**, 579 (2005).
- ³⁰C. Ganter and W. Schirmacher, [arXiv:1003.2514](https://arxiv.org/abs/1003.2514), *Philos. Mag.* (to be published).

- ³¹For example, $\Sigma''(k \rightarrow \infty, s) \propto s^{(d-2)/2}$ is required for a correct low-frequency behavior of the density of states in the scalar phonon model.
- ³²Without some nontrivial balancing mechanism, which, however, would have to be proven.
- ³³W. Schirmacher, G. Ruocco, and T. Scopigno, *Phys. Rev. Lett.* **98**, 025501 (2007).
- ³⁴W. Schirmacher, *Europhys. Lett.* **73**, 892 (2006); B. Schmid and W. Schirmacher, *Phys. Rev. Lett.* **100**, 137402 (2008); W. Schirmacher, B. Schmid, C. Tomaras, G. Viliani, G. Baldi, G. Ruocco, and T. Scopigno, *Phys. Status Solidi C* **5**, 862 (2008). In the latter paper the role of a correlation length in $K(k)$ is explored.
- ³⁵B. Movaghar and W. Schirmacher, *J. Phys. C* **14**, 859 (1981).
- ³⁶C. Ganter and W. Schirmacher, *Philos. Mag. B* **81**, 915 (2001).
- ³⁷W. Schirmacher, G. Diezemann, and C. Ganter, *Physica B* **284-288**, 1147 (2000).
- ³⁸J. Horbach, W. Kob, and K. Binder, *Eur. Phys. J. B* **19**, 531 (2001).
- ³⁹A. Akhiezer, *J. Phys. (Moscow)* **1**, 277 (1939).
- ⁴⁰P. B. Allen and J. L. Feldman, *Phys. Rev. B* **48**, 12581 (1993); J. L. Feldman, M. D. Kluge, P. B. Allen, and F. Wooten, *ibid.* **48**, 12589 (1993).
- ⁴¹C. Tomaras, B. Schmid, and W. Schirmacher, *Phys. Rev. B* **81**, 104206 (2010).
- ⁴²C. Masciovecchio, G. Baldi, S. Caponi, L. Comez, S. Di Fonzo, D. Fioretto, A. Fontana, A. Gessini, S. C. Santucci, F. Sette, G. Viliani, P. Vilmercati, and G. Ruocco, *Phys. Rev. Lett.* **97**, 035501 (2006).
- ⁴³A. Devos, M. Foret, S. Ayrinhac, P. Emery, and B. Rufflé, *Phys. Rev. B* **77**, 100201 (2008).
- ⁴⁴G. Baldi, V. M. Giordano, G. Monaco, and B. Ruta, *Phys. Rev. Lett.* **104**, 195501 (2010).
- ⁴⁵B. Rufflé, S. Ayrinhac, E. Courtens, R. Vacher, M. Foret, A. Wischnewski, and U. Buchenau, *Phys. Rev. Lett.* **104**, 067402 (2010).
- ⁴⁶A. Christou and R. B. Stinchcombe, *J. Phys. C* **19**, 5895 (1986).